In vivo continuous and simultaneous monitoring of brain energy substrates with a multiplex amperometric enzyme-based biosensor device

De Lima Braga Lopes Cordeiro, Carlos; de Vries, M.G.; Ngabi, W; Oomen, P.E.; Cremers, T.I.F.H.; Westerink, B.H.C.

Published in:
Biosensors and Bioelectronics

DOI:
10.1016/j.bios.2014.09.101

Publication date:
2015

Biosensors and Bioelectronics 67 (2015) 677–686

Contents lists available at ScienceDirect

Biosensors and Bioelectronics

journal homepage: www.elsevier.com/locate/bios

In vivo continuous and simultaneous monitoring of brain energy substrates with a multiplex amperometric enzyme-based biosensor device

C.A. Cordeiro [a,b,*], M.G. de Vries [a], W. Ngabi [b], P.E. Oomen [a], T.I.F.H. Cremers [a,b,c], B.H.C. Westerink [a,b]

[a] Brains On-Line BV, Groningen, the Netherlands
[b] University of Groningen Institute of Pharmacy, Groningen, the Netherlands
[c] Brains On-Line LLC, San Francisco, California, USA

ARTICLE INFO

Article history:
Received 7 June 2014
Received in revised form
27 August 2014
Accepted 22 September 2014
Available online 16 October 2014

Keywords:
In vivo
Multiplex
Real-time
Continuous biomonitoring
Amperometric
Enzyme-based

ABSTRACT

Enzyme-based amperometric biosensors are widely used for monitoring key biomarkers. In experimental neuroscience there is a growing interest in *in vivo* continuous and simultaneous monitoring of metabolism-related biomarkers, like glucose, lactate and pyruvate. The use of multiplex biosensors will provide better understanding of brain energy metabolism and its role in neuropathologies such as diabetes, ischemia, and epilepsy.

We have developed and characterized an implantable multiplex microbiosensor device (MBD) for simultaneous and continuous *in vivo* monitoring of glucose, lactate, and pyruvate.

First, we developed and characterized amperometric microbiosensors for monitoring lactate and pyruvate. *In vitro* evaluation allowed us to choose the most suitable biosensors for incorporation into the MBD, along with glucose and background biosensors. Fully assembled MBDs were characterized *in vitro*. The calculated performance parameters (LOD, LR, LRS, I_{MAX} and $_{app}K_M$) showed that the multiplex MBD was highly selective and sensitive (LRS $\geq$ 100 nA/mM) for each analyte and within an adequate range for *in vivo* application.

Finally, MBDs were implanted in the mPFC of anesthetized adult male Wistar rats for *in vivo* evaluation. Following an equilibration period, baseline brain levels of glucose (1.3 ± 0.2 mM), lactate (1.5 ± 0.4 mM) and pyruvate (0.3 ± 0.1 mM) were established. Subsequently, the MBDs recorded the responses of the animals when submitted to hyperglycemic (40% glucose i.v.) and hypoglycemic (5 U/kg insulin i.v.) challenges. Afterwards, MBDs were recalibrated to convert electrochemical readings into accurate substrate concentrations and to assess biofouling. The presented MBD can monitor simultaneously multiple biomarkers *in vivo*.

1. Introduction

The brain has high energy demands. Despite accounting for only 2% of the total body mass, it requires up to 25% of the total glucose consumption (Brady et al., 2006; Genc et al., 2011). Its high requirements are dependent on a continuous flow of energy substrates from the circulating blood (Du et al., 2012), and the activation of discrete brain areas is directly related to increases in energy requirements and in glucose utilization (Duelli and Kuschinsky, 2001; Fox et al., 1988).

According to the classical view on brain energy metabolism, glucose is the predominant energy substrate for both neurons and glial cells, followed at lesser extent by ketone bodies and monocarboxylic acids like pyruvate and lactate (Vannucci et al., 1997). While ketone bodies are of great importance in early development stages, pyruvate and lactate seem to have a role in the adult brain (Vannucci and Simpson, 2003). Classical neuroenergetics state that lactate produced in the glycolisis is released into the extracellular fluid and metabolized to prevent damage to adjacent cells. In contrast, pyruvate is regarded solely as mediator in glucose metabolism (Sokoloff, 1977).

* Corresponding author at: Brains On-Line BV, De Mudden 16 9747, AW Groningen, The Netherlands.
E-mail address: carlos.cordeiro@brainsonline.org (C.A. Cordeiro).

http://dx.doi.org/10.1016/j.bios.2014.09.101
0956-5663/

Advances in the technology for monitoring neuroenergetics have provided evidence that challenges this view (Drevets et al., 2002; El Hage et al., 2011; Erlichman et al., 2008; Hertz et al., 2007). Increases in blood flow and brain glucose utilization, in response to increases in energy requirements, are not matched by parallel increases in oxygen consumption, necessary for full glucose metabolism dependency (Fillenz and Lowry, 1998; Hertz et al., 2007; Kiyatkin and Lenoir, 2012; Leegsma-Vogt et al., 2003; Lowry et al., 1998a; Lowry and Fillenz, 1997). Moreover, it was found that lactate can readily be taken up and oxidized in both neurons and astrocytes, and can even sustain neuronal activity in glucose absence (Bouzier-Sore et al., 2003). These and other insights have led to the postulation of alternative views on neuroenergetics, with the astrocyte-neuron lactate shuttle (ANLS) hypothesis the most studied (Pellerin 2010; Pellerin and Magistretti, 1994).

The ANLS states that glia cells and lactate play an unprecedented active role in brain energy metabolism. In the astrocyte, glucose is metabolized to pyruvate, which can have two fates. Whilst part of it is used to produce energy for the astrocyte itself, the remaining pyruvate is converted into lactate and released into the extracellular fluid, to be taken up by surrounding neurons (Allaman et al., 2011; Dienel, 2011; Halim et al., 2010).

Disturbances of the regulation of brain energy metabolism have been related to impairments in the cognitive processes of learning and memory (Hertz and Gibbs, 2009; Kapogiannis and Mattson, 2011) and are involved in several neuropathologies. Deregulation of either glucose levels or the lactate/pyruvate ratio are associated with neuropathologies such as epilepsy (Cloix and Hévor, 2009), meningitis (Ginsberg, 2004; Komorowski et al., 1978; van de Beek et al., 2006), ischemia (Berthet et al., 2009; Tokumaru et al., 2009) and affective disorders (Li et al., 2010; Moretti et al., 2003; Pratt et al., 2008). Additionally, there is evidence that changes in glucose and lactate brain levels affect glucose homeostasis and diabetes (Ahmad et al., 2008; Marino et al., 2011; Marty et al., 2007; McCrimmon, 2012; Ramnanan et al., 2013; Routh, 2010; Thorens, 2010; Watts and Donovan, 2010).

Biomonitoring of glucose, lactate and pyruvate is fundamental for understanding and treatment of these pathologies. The existing technology allows us to understand that glucose and lactate levels are higher than pyruvate levels, both in humans and animal models. While glucose and lactate are within the millimolar range (between 1 and 2 mM) (Ahmad et al., 2008; Gramsbergen et al., 2004; Leegsma-Vogt et al., 2001; Lin et al., 2009; Lowry et al., 1998a; Rocchitta et al., 2013), pyruvate brain levels are significantly lower (circa 200 μM) (Schulz et al., 2000; Wagner et al., 2005). However, these values depend on many factors, most related to the analytical method employed, each with their advantages and drawbacks.

State of the art technology for brain biomonitoring include invasive and non-invasive techniques. Ideally, biomonitoring of target analytes should be performed by non-invasive methods such as positron emitting tomography (PET), magnetic resonance imaging (MRI) and magnetic resonance spectroscopy (MRS). However, these methods have severe limitations characterized by low quantitative resolution and limited temporal and/or spatial resolution (Byrnes et al., 2014; Haller et al., 2014; Lang et al., 2014; Li et al., 2013). Therefore invasive methods such as microdialysis and microbiosensors are needed for additional *in situ* information, such as basal levels and dynamic changes of each analyte in a discrete brain area.

Although microdialysis allows biomonitoring of multiple analytes with a high spatial resolution (mm), it still lacks the needed temporal resolution to monitor the expected fast changes in brain energy metabolism. Biosensors can combine spatial (μm) and temporal (≤ 1 s) resolution with high selectivity, rapid response time and ease of miniaturization. These features make these devices very appealing for *in vivo* biomonitoring of brain energy biomarkers.

A wide variety of biosensors have been successfully used for *in vivo* biomonitoring (Wang, 1999; Wilson and Gifford, 2005). However, in biomedical applications, experimental neuroscience in particular, amperometric enzyme-based biosensors have arguably been the most successful. Amperometric enzyme-based biosensors rely on the oxidation of an electroactive product (often H_2O_2) of an enzymatic reaction (typically mediated by oxidases) at the electrode surface (Thévenot et al., 1999). However, at the working potentials necessary to oxidize the electroactive molecules of interest (>500 mV), other electroactive compounds are prone to be oxidized, resulting in non-specific electrochemical interference (Lowry et al., 1998b; Wahono et al., 2012). The incorporation of permselective membranes (e.g. Nafion and Poly (Phenylenediamine) (PPD)) is often used to overcome electrochemical interference (Moatti-Sirat et al., 1994; Moussy et al., 1993; O'Neill et al., 2008). Besides increasing biosensor selectivity, these membranes minimize electrode passivation, a biofouling effect (Wisniewski et al., 2000). Although its impact is bigger in chronic cases, biofouling can be observed even in acute implantations (Koschwanez and Reichert, 2007; Wisniewski et al., 2000; Wisniewski and Reichert, 2000).

These type of biosensors were successfully applied for *in vivo* biomonitoring of neurotransmitters (Mitchell, 2004; Oldenziel et al., 2006; Pomerleau et al., 2003; Wahono et al., 2012) and energy biomarkers (Ahmad et al., 2008; Calia et al., 2009; Gramsbergen et al., 2004; Leegsma-Vogt et al., 2003; Lowry et al., 1998b; Roche et al., 2011; Vasylieva et al., 2011). Simultaneous monitoring of glucose and lactate has already been successfully described, even coupled to a telemetric device (Rocchitta et al., 2013). Unfortunately, the device did not allow the necessary spatial resolution needed for biomonitoring in a discrete brain area. The attempt of combining glucose, lactate and pyruvate biosensors into a single device, for *in vivo* real-time simultaneous monitoring of these analytes within a discrete brain area is an original application.

Here we describe the development and characterization of a novel multiplex biosensor device (MBD) for *in vivo* real-time continuous and simultaneous *in vivo* monitoring of glucose, lactate and pyruvate. *In vitro* electrochemical evaluation allowed us to choose the most suitable lactate and pyruvate biosensors to be incorporated in MBD, along with a glucose biosensor. Fully assembled MBDs were electrochemically evaluated *in vitro* prior to assess its suitability for *in vivo* implantation. After the MBDs were implanted in the medial prefrontal cortex (mPFC) of anesthetized adult Wistar rats. Following an equilibration period, animals were submitted to hyperglycemia (40% glucose i.v.) and hypoglycemia (5 U/kg insulin i.v.) challenges. Subsequently, the MBDs were explanted and recalibrated to convert electrochemical readings into accurate glucose, lactate and pyruvate levels and to assess biofouling.

2. Materials and methods

2.1. Materials

Glucose oxidase (GO*x*) (EC 1.1.3.4) from *Aspergillus niger* and Lactate oxidase (LO*x*) (EC 1.13.12.4) from *Pediococcus sp*, bovine serum albumin (BSA), glutaraldehyde (GA), *m*-phenylenediamine (*m*PD), glucose, (L)-lactic acid, sodium pyruvate, ascorbic acid (AA), uric acid (UA), dopamine (DA) and 3.4-dihydroxiphenylacetic (DOPAC) were purchased from Sigma-Aldrich (Schnelldorff, Germany). Pyruvate oxidase (POx) (PYO 311) (EC 1.2.3.3) was

purchased from Sorachim (Lausanne, Switzerland). Platinum and silver wires (Ø200 μm) were obtained from Advent Research Materials. Hydrogen peroxide (35% wt) was obtained from Janssen Chimica (CA, United States of America). Insulin (Humulin R) 100 IU/ml was purchased from Eli Lilly (IN, USA). Phosphate buffer solution (PBS) was used containing: 145 mM Na^+, 1.2 mM Ca^{2+}, 2.7 mm K^+, 1.0 mM Mg^{2+}, 152 mm Cl^-, and 2.0 mM phosphate in ultrapurified water, brought to pH 7.4 with sodium hydroxide and degassed before use. UV curable glue (Uv Permacol UV ELC 2722) was purchased from Permacol BV (Ede, The Netherlands). Polycarilonitrile (PAN), PAN-10 membranes were purchased from Asahi-Kasei (China) Co. Ltd (Shanghai, China). Polyethersulfone (PE) MicroPES TF10 membranes, were purchased from Membrana (Wuppertal, Germany).

2.2. Multiplex biosensor device (MBD) assembly

Needle-type platinum microelectrodes (0.2 mm Ø × 1 mm long) were prepared as described by Wahono et al. (2012). After its assembly, microelectrodes surface was functionalized, based on a "layer-by-layer" (LBL) method (Zhao et al., 2006), and they were converted into glucose, lactate, pyruvate or BG biosensors.

2.2.1. Membrane assembly

Microelectrode surfaces were initially functionalized with a permselective membrane (P*m*PD) and sub sequentially modified with an hydrogel comprising an enzyme (either GO*x*, LO*x*, or PO*x*) cross-linked with GA and BSA. Fully assembled biosensors were allowed to cure for 48 h prior to calibration. To some lactate biosensors, (LO*x* 0.4 U/μL) a derivation of the classical LBL method was employed. We applied an additional hollow membrane (either PE or PAN). The procedures for membrane assembly were as below:

2.2.1.1. PmPD. P*m*PD was applied by cyclic voltammetry. Electropolymerization was carried in presence of 5 mM of P*m*PD in 100 mM PBS pH 7.4. For electrodeposition all electrodes were submitted to the same cyclic voltammetry protocol with a scan from +200 to +700 mV at a scan rate of 20 mV/s over 200 cycles (Wahono et al., 2012). After, the membrane was cured for 24 h at room temperature.

2.2.1.2. Enzymatic hydrogel. Microelectrodes functionalized with P*m*PD were coated manually under an optical microscope with an hydrogel of either GO*x* (0.2 U/μL), LO*x* (0.2; 0.4 or 0.8 U/μL) or PO*x* (0.2; 0.4 or 0.8 U/μL) cross-linked with GA and BSA. Biosensors were coated 25 times and allowed to cure for 48 h prior to calibration.

2.2.1.3. Outer membrane assembly. Following assembly of the membranes, to some lactate biosensors an outer membrane was applied. A hollow microdialysis membrane (1 mm long), either PE or PAN, was applied on top of fully assembled biosensors.

2.2.2. Implantable device assembly

The multiplex biosensor device (MBD) comprised an array of four biosensors (glucose, lactate, pyruvate and BG). Each biosensor was then coupled to a copper wire and assembled in pairs in two separate microdialysis probe bodies (Brainlink, The Netherlands) sealed by UV curable glue (Fig. 1). The MBD tip Ø was approximately 0.85 mm^2.

2.3. In vitro calibration

2.3.1. Pre calibration

Pre-calibrations of both individual sensors and MBD were carried out in PBS (pH 7.4) at 700 mV *vs.* Ag/AgCl using a 4-channel potentiostat (Pinnacle, model 3104 Pinnacle Tech. Inc., USA) and according to the procedure described by Wahono et al. (2012). All interference compounds (DA 2 μM; DOPAC 20 μM; UA 50 μM; AA 250 μM) were added to the solution prior to consecutive additions of the target analyte (either lactate or pyruvate or glucose) from 0.02 up to 8 mM (0.02; 0.05; 0.1; 0.2; 0.5; 1; 2; 4 and 8 mM) followed by consecutive additions of H_2O_2 (50, 100 and 200 μM). Noise and limit of detection (LOD) were calculated by linear regression, whereas linear range (LR), linear range slope (LRS), apparent Michaelis–Menten constant ($_{app}K_M$) and maximum current intensity (I_{Max}) were calculated using non-linear regression.

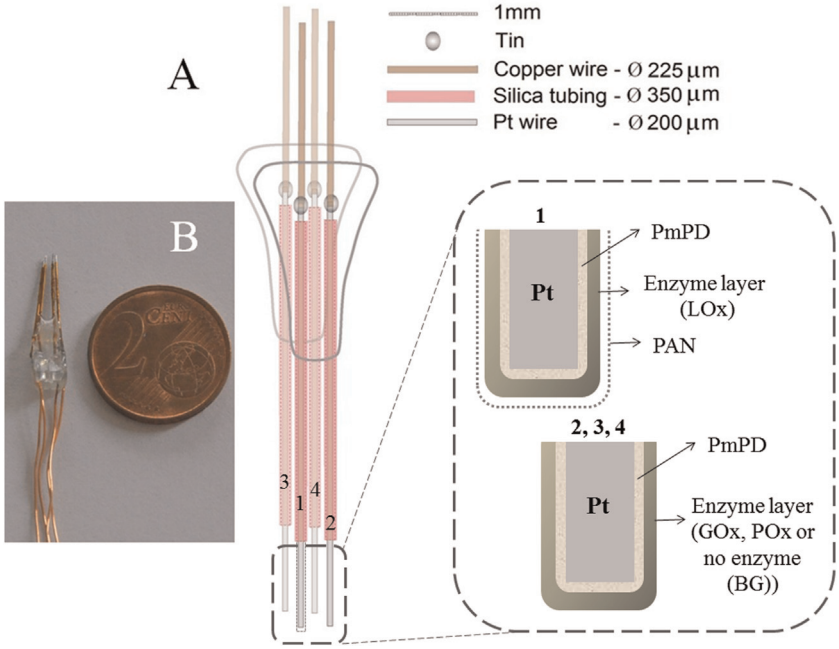

Fig. 1. (A) Schematic representation of the MBD 1 – Lactate Biosensor; 2 – Glucose Biosensor, 3 – Pyruvate biosensor, 4 – Background sensor (BG). Inset – Schematic representation of the microelectrode tips of the biosensors included in the MBD. (B) Fully assembled MBD (the coin (2.5 cm Ø) is shown for size comparison).

2.3.2. Post-calibration

The biosensors incorporated in the MBD were recalibrated immediately after the *in vivo* experiments in PBS (pH 7.4) at 700 mV *vs.* Ag/AgCl to evaluate biofouling. The currents obtained by each biosensor during the *in vivo* experiment were converted in final analyte concentrations, based on the analytical parameters calculated from the post-calibration.

2.4. In vivo experiments

Male Wistar rats (350–425 g) were used in all *in vivo* experiments. Animals were individually housed in Plexiglas cages prior to the experiment. All experiments were performed under anesthesia (isoflurane/O_2). All animals were submitted to surgery to implant a jugular vein catheter (for frequent blood sampling and compound administration) and to implant the MBD in the mPFC; AP+3.4 mm; ML+0.8 mm; VD−5.0 mm relative to bregma, according to the stereotaxic atlas (Paxinos and Watson 1986). All *in vivo* electrochemical measurements were performed at a constant potential, 700 mV vs. Ag/AgCl. Implantation was followed by a period of electrochemical signal equilibration (2 h) followed by pharmacological intervention for induction of glucose changes. Glucose levels were experimentally modulated by consecutive intravenous administration of vehicle (saline 1 ml/kg), glucose (20% w/V in saline) and insulin (5 U/kg) at intervals of 45 min, as previously described (Moon et al., 2013). Blood glucose was assessed at intervals of 15 min. Blood glucose values were obtained by colorimetric glucose strips (AccuChek; Roche). Animals were sacrificed immediately after the experiment by i.v. administration of pentobarbital. The MBD electrochemical signal was acquired at a rate of 10 H_Z and averaged.

All animal experiments were approved by the Institutional Animal Care and Use Committee of the University of Groningen.

2.5. Data analysis

Analytical and kinetic parameters were calculated by non-linear regression using GraphPad Prism 5.0. The calculated parameters include limit of detection (LOD), linear Range (LR) linear range slope (LRS) Michalis–Menten constant ($_{app}K_M$), maximum current intensity (I_{MAX}), and the surface independent constants (SI $_{app}K_M$, SI I_{MAX}). All data was presented as mean ± standard error of the mean (SEM). All calculated parameters were statistically evaluated either by One-Way or Two-Way ANOVA. When necessary, additional Bonferroni tests were performed. $p < 0.05$ and $p < 0.001$ were considered statistically significant and highly significant, respectively. Correlation analysis was performed using the Pearson Product Moment Correlation. All statistical analysis were performed using SigmaStat 12.0.

3. Results and discussion

3.1. Development of the lactate and pyruvate biosensors

Initially, we developed and characterized lactate and pyruvate needle-type enzyme-based amperometric biosensors *in vitro*. Enzyme loading was described as one of the major factors affecting biosensor properties (O'Neill et al., 2008). To reach a biosensor suitable for *in vivo* implantation, we constructed biosensors with similar geometry but loaded with different enzyme concentrations.

In vitro evaluation (Fig. 2) revealed that all biosensors were responsive to the tested concentrations of the target analytes (0.02–8 mM), displaying clear Michaelis–Menten kinetics. Both lactate and pyruvate biosensors displayed high linearity ($R^2 \geq 0.99$) for low analyte concentrations (up to 1 mM). We have calculated the most relevant analytical and kinetic parameters for biosensors, using a simplified Michaelis–Menten model for biosensors (O'Neill et al., 2008). Results are shown in Table 1.

Our results show a low LOD (≤ 5 μM) for all biosensors, independent of the enzyme and its loading concentration. Lactate biosensors coated with 0.8 U/μL displayed a LOD of 0.55 ± 0.05 μM, better than the optimal LOD reported in literature (Lin et al., 2009). The presented LOD values suggest that, once implanted, any developed biosensor would be able to monitor small changes in analyte levels in the brain of rodents.

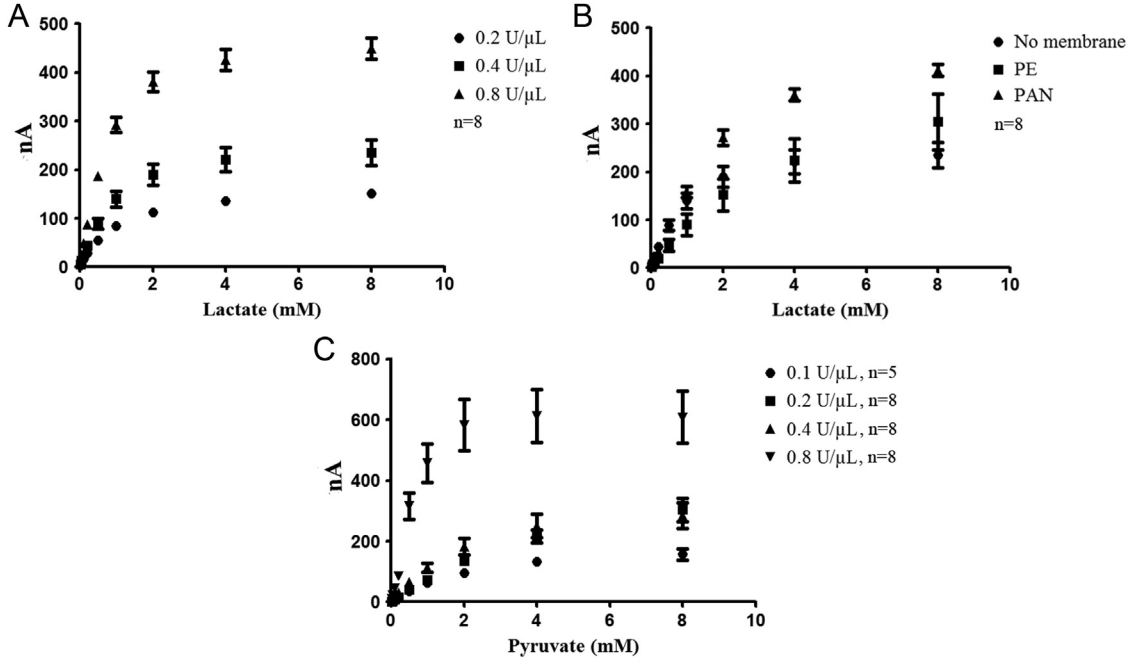

Fig. 2. Calibration curves of needle type enzyme based amperometric biosensors for *in vivo* monitoring of lactate (without (A) and with outer membrane (B)) and pyruvate (C) loaded with different enzyme concentration. Data are mean ± SEM.

Table 1
Calculated *in vitro* analytical and kinetic parameters for lactate (A) and pyruvate (B) biosensors. These include limit of detection (LOD), apparent Michaelis–Menten constant ($_{app}K_M$), surface independent apparent Michaelis–Menten constant, (SI $_{app}K_M$), maximum current (I_{MAX}), surface independent maximum current (SI I_{MAX}), linear range (LR) and linear range slope (LRS). Data are mean ± SEM.

A	Outer Membrane	*None*						*PE*		*PAN*	
	LOx (U/μL)	***0.2***		***0.4***		***0.8***		***0.4***		***0.4***	
	n	8		8		8		8		8	
		Mean	***SEM***	***Mean***	***SEM***	***Mean***	***SEM***	***Mean***	***SEM***	***Mean***	***SEM***
	LOD_{Lac} (μM)	1.48	0.23	2.92	0.54	0.55	0.05	4.63	2.17	0.86	0.21
	$_{app}K_M$ (mM)	1.04	0.11	0.94	0.20	0.80	0.08	4.16	1.76	2.26	0.20
	SI $_{app}K_M$ (mM)	0.98	0.09	0.89	0.20	0.80	0.12	N/A	N/A	N/A	N/A
	I_{Max} (nA)	170.80	5.82	269.30	17.42	509.60	14.44	461.90	95.43	544.50	19.47
	SI I_{Max}	0.12	0.003	0.24	0.02	0.30	0.01	N/A	N/A	N/A	N/A
	LR (mM)	0.52	0.06	0.47	0.10	0.40	0.04	2.08	0.88	1.13	0.10
	LRS_{Lac} (nA/ mM)	164.87	52.35	286.00	88.49	634.15	188.29	111.11	54.17	241.14	96.43
B	POx (U/μL)	***0.1***		***0.2***		***0.4***		***0.8***			
	n	5		8		8		8			
		Mean	***SEM***	***Mean***	***SEM***	***Mean***	***SEM***	***Mean***	***SEM***		
	LOD_{Pyr} (μM)	5.60	1.94	1.37	0.23	2.51	0.58	1.61	0.54		
	$_{app}K_M$ (mM)	2.22	0.41	2.23	0.57	5.88	1.56	0.69	0.19		
	SI $_{app}K_M$ (mM)	2.16	0.10	2.94	0.43	4.77	0.74	0.71	0.21		
	I_{Max} (nA)	200.50	14.20	362.30	34.93	527.80	76.40	714.70	55.00		
	SI I_{Max}	0.11	0.002	0.26	0.02	0.20	0.02	0.59	0.05		
	LR (mM)	1.11	0.28	1.09	0.31	2.86	1.10	0.35	0.11		
	LRS_{Pyr} (nA/ mM)	90.40	33.82	162.76	60.89	89.73	48.99	1030.12	294.65		

3.1.1. Lactate biosensors

An increase in LO*x* loading resulted in significant differences in biosensor performance (Table 1-A). Biosensors loaded with 0.8 U/μL of LO*x* displayed the highest values for both I_{MAX} and SI I_{MAX} (509.60 ± 14.40 nA and 0.30 ± 0.01 respectively *vs.* all, $p \leq 0.001$) Additionally, biosensors coated with 0.8 U/μL also displayed higher LRS than any other lactate biosensor (634.15 ± 188.29 nA/mM, $p \leq 0.05$). However, changes in enzyme concentration did not induce any changes in biosensor affinity ($_{app}K_M$), enzyme affinity (SI $_{app}K_M$) or LR.

However, physiological relevant levels of brain lactate are higher than the LR of any of the tested lactate biosensors (Lin et al., 2009; Rocchitta et al., 2013). The low LR observed most likely compromise the ability of these biosensors to accurately detect *in vivo* lactate increases.

The LR can be expanded without compromising LRS by the application of an outer membrane, which will function as an additional diffusion barrier (Rocchitta et al., 2013). Although outer membranes are typically self-assembled monolayers on top of the existing enzymatic membrane (Nafion or polyurethane) (Moussy et al., 1993; Vaddiraju et al., 2011), the use of hollow microdialysis membranes in *in vivo* biosensor applications has also been reported (Koh et al., 2011; Leegsma-Vogt et al., 2001, 2003). In addition, the use of a membrane on top of the enzyme layer is an effective anti-biofouling strategy (Wisniewski and Reichert, 2000).

We have applied two different microdyalisis membranes in the assembly of lactate biosensors loaded with 0.4 U/μL. The incorporation of an outer membrane resulted in an increase in $_{app}K_M$ LR and I_{MAX}, independent of the type of membrane applied without compromising LRS. Lactate biosensors with an outer membrane (PE or PAN) displayed a significantly higher I_{MAX}, when compared with biosensors without an additional membrane (461.90 ± 95.43 and 544.50 ± 19.47 nA respectively vs. 269.30 ± 17.42 nA, p<0.05). Electrochemical biosensors whose enzyme is immobilized by cross-linking with GA, suffer from enzyme loss upon immersion in buffer (House et al., 2007). The use of any outer membrane prevented enzyme loss, enabling an higher I_{MAX}. The $_{app}K_M$ and LR of biosensors with PES or PAN were 2-fold and 3-fold higher respectively when compared with biosensors with no outer membrane. Despite a significant increase in LR when compared with biosensors without a membrane (1.13 ± 0.10 *vs.* 0.47 ± 0.10 mM, $p < 0.05$), it was still considered low for *in vivo* applications. Therefore we chose biosensors loaded with 0.4 U/μL with the addition of PAN as the most suitable to be incorporated in an MBD for *in vivo* application. These biosensors displayed a higher I_{MAX} and LRS than reported lactate biosensors for *in vivo* application (Rocchitta et al., 2013).

3.1.2. Pyruvate biosensors

Loading biosensors with different PO*x* concentrations resulted in significant changes in biosensor performance. Pyruvate biosensors loaded with 0.8 U/μL of PO*x* displayed higher I_{MAX} than biosensors loaded with either 0.1 or 0.2 U/μL (714.7 ± 55.2 *vs.* 362.3 ± 34.9 and 200.5 ± 14.2 nA respectively, $p < 0.001$) but not biosensors loaded with 0.4 U/μL. Moreover we have found that biosensors loaded with 0.8 U/μL displayed an SI I_{MAX} higher than any other biosensor configuration (0.59 *vs.* all, $p < 0.001$), while biosensors loaded with 0.1 U/μL had the lowest SI I_{MAX} (0.11 ± 0.002 *vs.* all, $p < 0.001$). The increase the amount of pyruvate oxidase reticulated within the hydrogel resulted in an increase of biosensor catalytic activity.

Biosensors loaded with 0.8 U/μL displayed the highest affinity for pyruvate. Its $_{app}K_M$, SI $_{app}K_M$ and LR were significantly lower than biosensors loaded with 0.4 U/μL of PO*x* (0.69 ± 0.19 *vs.* 5.88 ± 1.56 mM p<0.001). Differences observed in both catalytic activity and biosensor affinity resulted in significant differences in LRS. Biosensors loaded with 0.8 U/μL of PO*x*, displayed the highest LRS (1030.12 ± 294.65 nA/mM *vs.* all, $p < 0.001$).

Although biosensors loaded with 0.8 U/μL of PO*x* displayed the highest LRS and I_{MAX}, were not considered suitable for *in vivo* implantation. Their LR was very close to the expected levels of pyruvate in the ECF. Therefore, we chose to include pyruvate

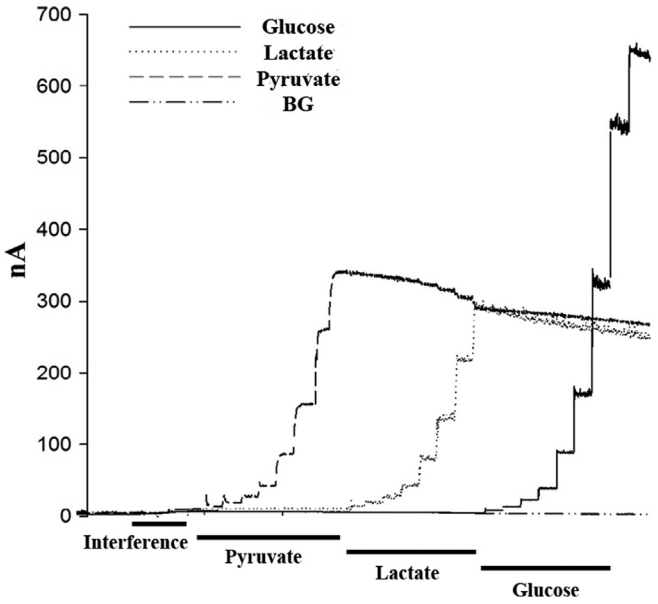

Fig. 3. Typical *in vitro* calibration of the MBD for simultaneous monitoring of the analytes of interest, glucose, lactate and pyruvate (20 μM to 8 mM) in presence of the major electrochemical interfering compounds: ascorbic acid (250 μM); uric acid (50 μM); dopamine (2 μM) and 3,4-dihydroxiphenylacetic acid (DOPAC) (20 μM).

biosensors loaded with 0.2 U/μL of PO*x* in the MBD. Although displaying lower LR and I_{MAX}, they did show higher LRS (162.76 ± 60.89 nA/mM) within a suitable LR (1.09 ± 0.31 mM).

3.2. *In vitro evaluation of the multiplex biosensor device*

All MBD were electrochemically evaluated *in vitro* to assess its ability to accurately monitor the target analytes simultaneously and independently. Increasing concentrations of pyruvate, lactate and glucose, in presence of the major electrochemical interference compounds, were added into a stirring beaker. Results are shown in Fig. 3.

None of the biosensors responded to the addition of any of the non-specific electroactive species and each biosensor responded selectively to the addition of the target analyte. For lactate and pyruvate biosensors the oxidation currents obtained were comparable to those observed for individual calibration. However, pyruvate biosensors responded to high non-physiological lactate concentrations (8 mM). This was a results of the conversion of lactate into pyruvate by the LO*x* immobilized in the surface of the lactate biosensor. No response was observed for any of the other concentrations. Additionally, the MBD was designed to allow enough physical separation of the biosensors when implanted, avoiding *in vivo* cross-over effects.

3.3. *Post-calibration*

After the experiment, the MBDs were explanted, and immediately placed in a beaker for post-calibration (Koschwanez and Reichert, 2007). Results obtained are displayed on Fig. 4.

All biosensors retained high selectivity and sensitivity after acute *in vivo* implantation. Nevertheless we have observed significant differences in some of the biosensors performance parameters. Our results suggest that although all biosensors were affected by biofouling, its extent was biosensor dependent.

In vivo implantation induced a severe increase (up to 5 fold, $p \leq 0.05$) in ${}_{app}K_M$ of the glucose biosensor. This decrease in affinity implied an extended LR, with an average decrease in LRS of about 50%. No differences were observed in I_{MAX}. The formation of a biofilm on top of the glucose biosensor might explain the decrease in affinity (Wisniewski et al., 2000), by creating an additional barrier for glucose diffusion.

Although no statistically significant changes were observed in most of the analytical parameters, pyruvate biosensors were also affected by biofouling. We have observed a dramatic decrease in I_{MAX} ($\geq$ 2fold, $p \leq 0.001$), suggesting a decrease in the amount of active enzyme. The fact that these biosensors were coated with an enzyme of bacterial source, and had no protective layer, might explain this reduction.

In general, lactate biosensors were the least affected by biofouling. However, we have noticed a non-significant reduction in the LRS when compared with pre-*in vivo* values. The use of a biocompatible outer microdyalisis membrane (PAN) used for the lactate sensors minimized the effects of biofouling. The use of outer membranes has been reported as an effective anti-biofouling method, especially for chronic implantations (Wisniewski and Reichert, 2000). Our results show that differences in biosensor geometry, resulted in significant differences of biofouling effects on biosensor performance.

Nonetheless, all of the biosensors incorporated within the MBD were still able to monitor small changes in all target analytes with high selectivity and sensitivity within a suitable range. Therefore the MBD was considered suitable for accurate monitoring of the respective analytes, thus validating *in vivo* application of the MBD.

3.4. *In vivo experiment*

To assess the ability of the MBD to continuously and simultaneously monitor glucose, lactate and pyruvate in the rat brain we implanted them in the mPFC of anesthetized animals. In addition we implanted a jugular vein catheter, for frequent blood sampling. After implantation, we have allowed biosensor equilibration prior to the beginning of the experiment.

Background biosensors reached a stable basal electrochemical signal after 30 min. Both glucose and pyruvate biosensor took about 30–45 min to stabilize. The delayed equilibration time observed for lactate biosensor ($>$ 60 min) can be explained by the use of the outer membrane, that formed an additional physical barrier, thereby reducing diffusion rate.

After equilibration, we ensured a stabilization period of 15 min, prior to any pharmacological intervention to assure biosensor stability and to assess basal levels of the target analytes (Fig. 4). Brain analyte levels were calculated using the performance parameters calculated based on the post-calibration.

3.4.1. *Basal glucose levels*

Resting blood glucose levels were 10 fold higher than brain glucose levels (12.01 ± 0.58 *vs.* 1.30 ± 0.14 mM, $p < 0.001$). Blood glucose levels in rats are typically around 5–6 mM (de Vries et al., 2003, 2005). However, in anesthetized animals these levels are reported to increase 2-fold (Moon et al., 2013).

Basal brain glucose levels are reported to range from 0.3 mM up to 2.5 mM. These values vary according to the conscious state of animal, type of anesthesia, and analytical method employed. Furthermore, there is evidence that points to regional differences in brain glucose levels (Duelli and Kuschinsky, 2001). Most of the brain glucose levels detected by biosensors refer to the striatum and to values between 0.3 and 0.7 mM (Ahmad et al., 2008; Fillenz and Lowry, 1998; Kiyatkin and Lenoir, 2012; Leegsma-Vogt et al., 2003; Lowry et al., 1998a). A recent study performed in anesthetized animals with a biosensor implanted in the mPFC describes basal levels of 0.68 mM (Vasylieva et al., 2011), which is roughly half of what we report (1.30 ± 0.14 mM). However, in the mentioned study, basal levels were calculated based on

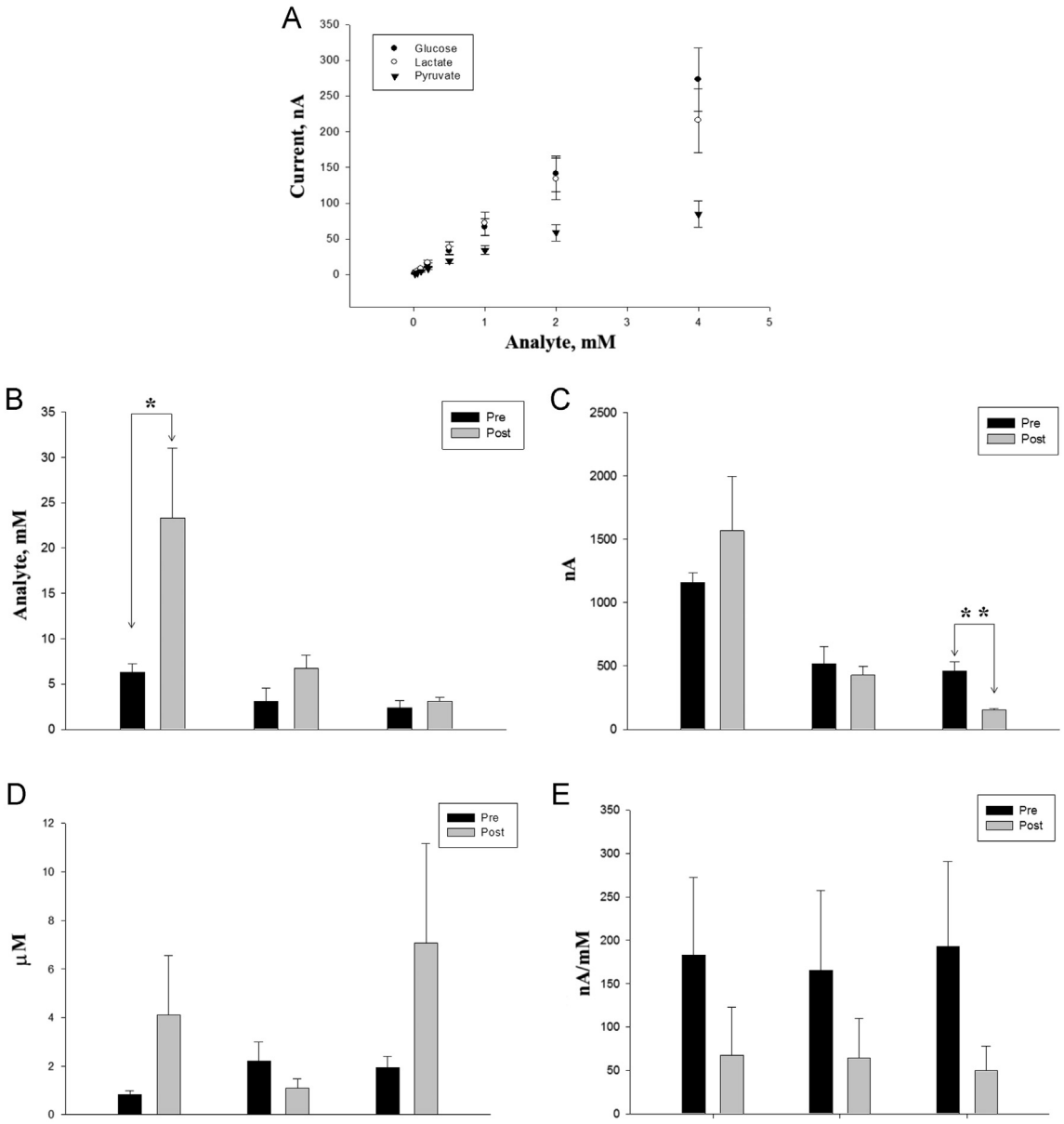

Fig. 4. Evaluation of relevant performance parameters of the biosensors incorporated within the MBD after *in vivo* implantation: (A) *In vitro* post-calibration; (B) $_{app}K_M$; (C) I_{MAX}; (D) limit of detection (LOD); and (E) linear range slope (LRS). Data are mean ± SEM.

pre-calibration data, using less sensitive (12.3 ± 3.8 pA/µM) biosensors.

3.4.2. Basal lactate levels

Since the 1970s brain lactate has been considered as an oxidative metabolic waste, not actively involved in brain energy metabolism. However, according to the ANLS, lactate plays an active role in brain energy metabolism (Pellerin, 2010). Literature on brain lactate reports levels that range from 0.3 to 2 mM. Brain lactate levels obtained by the lactate biosensor incorporated in the MBD (1.56 ± 0.48 mM) are higher than previously reported in biosensor studies (Fillenz and Lowry, 1998; Leegsma-Vogt et al., 2003; Lin et al., 2009; Lowry et al., 1998a), but lie within the large range of brain lactate levels reported in studies using standard methodologies.

3.4.3. Basal pyruvate levels

Here we report for the first time, to our knowledge, continuous monitoring of brain pyruvate, with biosensors. To date, information on brain pyruvate changes relied on microdialysis. Normal cerebrospinal fluid in humans values vary between 0.08 and 0.16 mM (Wagner et al., 2005), while resting brain levels range from 0.1 to 0.2 mM (Schulz et al., 2000). Our results show slightly higher basal brain pyruvate levels (0.29 ± 0.10 mM), which could be attributed to the combination of better accuracy and spatial resolution, compared to state of the art methods.

3.4.4. Vehicle administration

Vehicle administration (saline, 1 ml/kg) did not induce significant changes in the concentration of glucose, lactate or pyruvate (Fig. 5E).Accordingly, no changes were observed in blood glucose either.

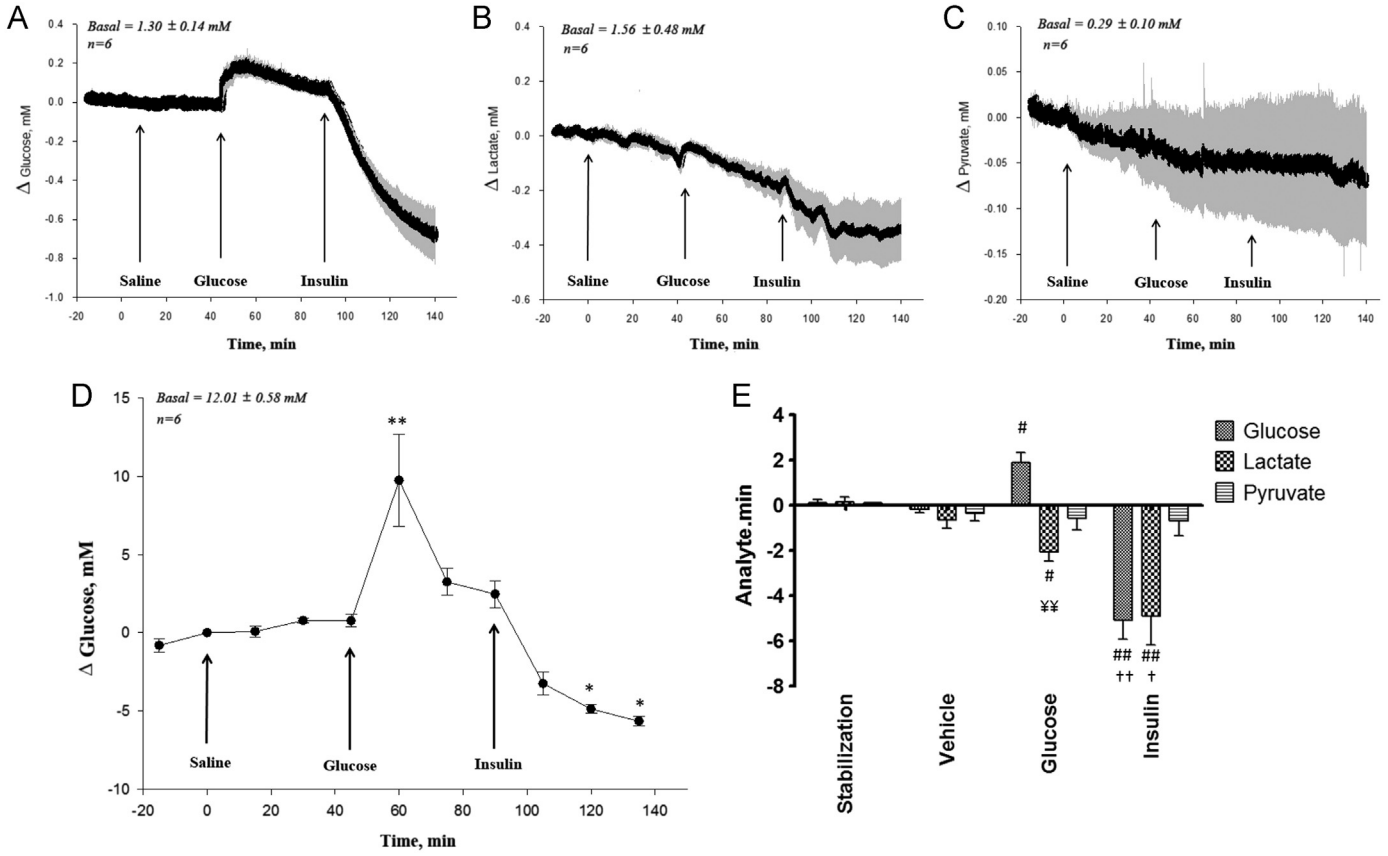

Fig. 5. *In vivo* continuous and simultaneous monitoring of changes in glucose (brain (A) and blood (D)), lactate (B) and pyruvate (C). Blood glucose levels are shown in (D). Effects of the administration of saline glucose (20% m/V) and insulin (5U/Kg) on its basal levels, expressed as areas under the curve (AUC) are shown in (E). * and ** indicate significant differences in blood glucose levels compared to $t=0$ min. # and ## indicate a significant difference compared to administration of vehicle ($p<0.05$ and $p<0.001$); ¥ and ¥¥ indicate a significant difference in induced changes between changes in glucose and lactate ($p<0.05$ and $p<0.001$); † and †† indicate a significant difference in changes induced by glucose and insulin administration ($p<0.05$ and $p<0.001$). Data are mean ± SEM.

3.4.5. Glucose administration

Glucose administration (20% m/V) induced a rapid increase in both brain and blood glucose levels ($p<0.05$ and $p<0.001$ respectively, at $t=60$) (Fig. 4A and E). Blood glucose increased about 10 mM and reached a maximum of 21.76 ± 2.93 mM, 15 min after administration ($t=60$) (Fig. 4D). After this peak, blood glucose declined and reached basal levels at $t=75$ min.

Brain glucose began to increase immediately after glucose administration. It reached its maximum levels (1.49 ± 0.05 mM) at $t=65$ min (Fig. 4B). Following this initial increase, brain glucose levels decreased transiently, although still significantly higher than basal glucose levels (all *vs.* 1.49 ± 0.05 $p<0.05$ from $t=62$ to $t=90$ min).

Although brain glucose can be produced in astrocytes by glycogenolysis (Di Nuzzo et al., 2011; Dienel, 2011; Hertz et al., 2013), most of the brain glucose is directly taken up from the circulating blood, facilitated by glucose receptors in the blood–brain barrier (BBB) (Duelli and Kuschinsky, 2001). Our results suggest a fast, but limited uptake of glucose by the brain in response to a sudden large increase in glucose in the blood stream. Apparently, the BBB acts as a buffer, keeping glucose levels within a narrow range, even if circulating blood glucose reaches extremely high levels.

Besides changes in brain glucose, administration of glucose in the blood stream induced small but significant changes in brain lactate levels (Fig. 4A and E). All MBD detected a fast decrease, followed by a sudden increase in brain lactate levels (Fig. 4B). The initial increase in lactate might be due to the activation of the brain, in response to a major event, such as the administration of a i.v. glucose bolus. A study combining biosensoring with brain stimulation, has shown a similar increase in brain lactate in response to activation of a discrete brain area (Hu and Wilson, 1997).

The activation of a brain area requires higher energy demand by the neurons located in that region. Rapid use of the lactate pool in the ECF could be responsible for the initial decrease in ECF lactate levels. Next, according to the ANLS, upon activation, release of glutamate by the neurons might trigger the production of lactate in the surrounding astrocytes. In turn lactate is released into the ECF and taken by the activated neurons. This would explain the increase in lactate levels following the initial decrease. These findings support the idea that lactate can sustain neuronal activity (Bouzier-Sore et al., 2003; Pellerin 2010).

In contrast, glucose administration did not induce any significant changes in brain pyruvate levels. According to both the classical view and ANLS, pyruvate is metabolized intracellularly for energy production (Pellerin 2010; Pellerin and Magistretti, 1994). Despite providing an excellent spatial resolution, the proposed device is only able to measure changes in the brain ECF, reaffirming both the classical view and the ANLS.

3.4.6. Insulin administration

We observed a pronounced decrease in brain glucose levels following i.v. insulin (5 U/kg) administration ($p<0.001$), which correlated well with changes in blood glucose (Pearson correlation coefficient 0.953, $p<0.05$). Brain glucose levels started to decrease immediately after the insulin administration ($t=90.5$ min) and continued to decrease at an apparent constant rate until the end of

the experiment. Brain glucose levels at the end of the experiment (0.62 ± 0.12 *vs.* 1.31 ± 0.14 mM, $p < 0.05$) were lower than basal levels ($p < 0.05$). A recent study, employing biosensors, showed that insulin administration did not influence glucose levels in the striatum (Ahmad et al., 2008). However, a similar decrease in glucose mPFC levels as presently reported in response to insulin (25 U/kg) administration has been noted (Vasylieva et al., 2011).

Interestingly, insulin induced a slight but significant increase in brain lactate (Fig. 5-E). Interestingly, the MBD was able to detect short-lasting increase in brain lactate, in response to insulin administration (from $t=90$ to $t=92$ min). After this steep increase, brain lactate levels started to decrease, reaching the lowest levels at $t=111$ min (1.19 ± 0.21 mM). Thereafter no changes in lactate levels were observed. Our data suggest the activation of the mPFC immediately after insulin administration, similar to what was observed following glucose administration. Surprisingly, changes in lactate displayed higher correlation with blood glucose, when compared with changes in brain glucose (Pearson correlation coefficient 0.992 *vs.* 0.953, $p < 0.001$). The role of insulin in brain glucose metabolism is still not clarified and biosensors might provide additional information to further understand its underlying mechanisms.

4. Conclusion

We developed and characterized an MBD for *in vivo* in real time simultaneous monitoring of the three major biomarkers in brain energy metabolism: glucose lactate and pyruvate.

The use of an MBD allowed us to accurately, continuously and simultaneously monitor glucose, lactate and pyruvate levels in a discrete brain area, with high spatial and temporal resolution. The MBD was able to measure the basal levels of glucose, lactate and pyruvate simultaneously. The high spatial resolution allowed us to monitor small and fast changes in brain levels of the target analytes, impossible to be tracked by state-of-the-art *in vivo* brain biomonitoring techniques

The use of the proposed MBD can increase the knowledge of the neuroenergetics fundamentals. It can lead to a clarification of the role of lactate, shed light on the putative ANLS hypothesis, but it may also reveal new therapeutic approaches in diseases related to brain energy metabolism.

References

Ahmad, F., Yusof, A.P.M., Bainbridge, M., Ghani, S.A., 2008. Biosens. Bioelectron. 23, 1862–1868.
Allaman, I., Belanger, M., Magistretti, P.J., 2011. Trends Neurosci. 34 (2), 76–87.
Berthet, C., Lei, H., Thevenet, J., Gruetter, R., Magistretti, P.J., Hirt, L., 2009. J. Cereb. Blood Flow Metab. 29, 1780–1789.
Bouzier-Sore, A.-K., Voisin, P., Canioni, P., Magistretti, P.J., Pellerin, L., 2003. J. Cereb. Blood Flow Metab. 23, 1298–1306.
Brady, S.T., Siegel, G.J., Albers, W.R., Price, D.L., 2006. Basic Neurochemistry: Principles of Molecular Cellular and Medical Neurobiology, 7th ed. Elsevier Academic Press, Burlington, MA, USA.
Byrnes, K.R., Jurgens, J.S., Wilson, C.M., Oakes, T.R., Brabazon, F., Selwyn, R.G., von Leden, R., 2014. Front. Neuroenergetics 5 (13), 1–24.
Calia, G., Rocchitta, G., Migheli, R., Puggioni, G., Spissu, Y., Bazzu, G., Mazzarello, V., Lowry, J.P., O'Neill, R.D., Desole, M.S., Serra, P.A., 2009. Sensors 9, 2511–2523.
Cloix, J.-F., Hévor, T., 2009. Curr. Med. Chem. 16, 841–853.
de Vries, M.G., Arseneau, L.M., Lawson, M.E., Beverly, J.L., 2003. Diabetes 52, 2767–2773.
de Vries, M.G., Lawson, M.A., Beverly, L.J., 2005. Am. J. Physiol. – Regul., Integr. Comp. Physiol. 289, R977–R981.
Di Nuzzo, M., Maraviglia, B., Giove, F., 2011. Bioessays 33, 319–326.
Dienel, G.A., 2011. J. Cereb. Blood Flow Metab. 30, 1893–1894.
Drevets, W.C., Bogers, W., Raichle, M.E., 2002. Eur. Neuropsychopharmacol. 12, 527–544.
Du, F., Zhang, Y., Zhu, X.-H., Chen, W., 2012. J. Cereb. Blood Flow Metab. 32, 1778–1787.
Duelli, R., Kuschinsky, W., 2001. News Physiol. Sci. 16, 71–76.
El Hage, M., Ferrier, B., Baverel, G., Martin, G., 2011. Neurochem. Int. 59 (8), 1145–1154.
Erlichman, J.S., Hewitt, A., Damon, T.L., Hart, M., Kurascz, J., Li, A., Leiter, J.C., 2008. J. Neurosci. 28 (19), 4888–4896.
Fillenz, M., Lowry, J.P., 1998. Exp. Physiol. 83, 233–238.
Fox, P.T., Raichle, M.E., Mintun, M.A., Dence, C., 1988. Science 241 (4864), 462–464.
Genc, S., Kurnaz, I.A., Ozilgen, M., 2011. BMC Syst. Biol. 5 (162), 1–13 (2011).
Ginsberg, L., 2004. Difficult and recurrent meningitis. J. Neurol. Neurosurg. Psychiatry 75 (Suppl. I), i16–i21.
Gramsbergen, J.B., Skjøth-Rasmussen, J., Rasmussen, C., Lambertsen, K.L., 2004. J. Neurosci. Methods 140, 93–101.
Halim, N.D., McFate, T., Mohyeldin, A., Okagaki, P., Korotchkina, L.G., Patel, M.S., Jeoung, N.-H., Harris, R.A., Schell, M.J., Verma, A., 2010. Glia 58 (10), 1168–1176.
Haller, S., Lovblad, K.-O., Giannakopoulos, P., Van De Ville, D., 2014. Brain Topogr. 29, 327–337.
Hertz, L., Gibbs, M.E., 2009. J. Neurochem. 1009 (Suppl.1), 10–16.
Hertz, L., Peng, L., Dienel, G.A., 2007. J. Cerebr. Blood Flow Metab. 27, 219–249.
Hertz, L., Xu, J., Song, D., Du, T., Yan, E., Peng, L., 2013. Front. Integr. Neurosci. 7 (20), 1–7.
House, J.L., Anderson, E.M., Ward, W.K., 2007. J. Diabetes Sci. Technol. 1 (1), 18–27.
Hu, Y., Wilson, G.S., 1997. J. Neurochem. 69, 1484–1490.
Kapogiannis, D., Mattson, M.P., 2011. Lancet Neurol. 10 (2), 187–198.
Kiyatkin, E.A., Lenoir, M., 2012. J. Neurophysiol. 108, 1669–1684.
Koh, A., Nichols, S.P., Schoenfisch, M.H., 2011. J. Diabetes Sci. Technol. 5 (5), 1052–1059.
Komorowski, R.A., Farmer, S.G., Hanson, G.A., Hause, L.L., 1978. J. Clin. Microbiol. 8 (1), 88–92.
Koschwanez, H.E., Reichert, W.M., 2007. Biomaterials 28 (25), 3687–3703.
Lang, S., Duncan, N., Northoff, G., 2014. Neurosurgery 74 (5), 453–465.
Leegsma-Vogt, G., Venema, K., Korf, J., 2003. J. Cerebr. Blood Flow Metab 23, 933–941.
Leegsma-Vogt, G., Venema, K., Postema, F., Korf, J., 2001. J. Neurosci. Res. 66, 795–802.
Li, C.-T., Wang, S.-J., Hirvonen, J., Hsieh, J.-C., Bai, Y.-M., Hong, C.-J., Liou, Y.-J., Su, T.-P., 2010. J. Affect. Disord. 127, 219.
Li, Q., He, X., Wang, Y., Liu, H., Xu, D., Guo, F., 2013. J. Biomed. Opt. 18 (10), 1–28.
Lin, Y., Zhu, N., Yu, P., Su, L., Mao, L., 2009. Anal. Chem. 81, 2067–2074.
Lowry, J.P., Demestre, M., Fillenz, M., 1998a. Dev. Neurosci. 20, 52–58.
Lowry, J.P., Fillenz, M., 1997. J. Physiol. 498 (2), 497–501.
Lowry, J.P., Miele, M., O'Neill, R.D., Boutelle, M.G., Fillenz, M., 1998b. J. Neurosci. Methods 79, 65–74.
Marino, J.S., Xu, Y., Hill, J.W., 2011. Trends Endocrinol. Metab. 22 (7), 275–285.
Marty, N., Dallaporta, M., Thorens, B., 2007. Physiology 22, 241–251.
McCrimmon, R.J., 2012. J. Clin. Endocrinol. Metabol. 97, 1–8.
Mitchell, K.M., 2004. Anal. Chem. 76, 1098–1106.
Moatti-Sirat, D., Poitout, V., Thom, V., Gangnerau, M.N., Zhang, Y., Hu, Y., Wilson, G. S., Lemonnier, E., Klein, J.C., Reach, G., 1994. Diabetologia 37, 610–616.
Moon, B.U., de Vries, M.G., Cordeiro, C.A., Westerink, B.H., Verpoorte, E., 2013. Anal. Chem. 85 (22), 10949–10955.
Moretti, A., Gorini, A., Villa, R.F., 2003. Mol. Psychiatry 8, 773–785.
Moussy, F., Harrison, D.J., O'Brien, D.W., Rajotte, R.V., 1993. Anal. Chem. 65, 2072–2077.
O'Neill, R.D., Lowry, J.P., Rocchitta, G., McMahon, C.P., Serra, P.A., 2008. Trends Anal. Chem. 27 (1), 78–88.
Oldenziel, W.H., Dijkstra, G., Cremers, T.I.F., Westerink, B.H., 2006. Brain Res. 118, 34–42.
Paxinos, G., Watson, C., 1986. The Rat Brain in Stereotacic Coordinates. Academic Press, London.
Pellerin, L., 2010. Diabetes Metab. 36, S59–S63.
Pellerin, L., Magistretti, P.J., 1994. Glutamate uptake into astrocytes stimulates aerobic glycolysis: a mechanism coupling neuronal activity to glucose utilization. Proc. Natl. Acad Sci. USA 91, 10625–10629.
Pomerleau, F., Day, B.K., Heuttl, P., Burmeister, J.J., Gerhardt, G.A., 2003. Ann. N.Y. Acad. Sci. 1003 (1), 454–457.
Pratt, J.A., Winchester, C., Egerton, A., Cochran, S.M., Morris, B.J., 2008. Br. J. Pharmacol. 153, S465–S470.
Ramnanan, C.J., Kraft, G., Smith, M.S., Farmer, B., Neal, D., Williams, P.E., Lautz, M., Farmer, T., Donahue, E.P., Cherrington, A.D., Edgerton, D.S., 2013. Diabetes 62 (1), 74–84.
Rocchitta, G., Secchi, O., Bazzu, G., Calia, G., Migheli, R., Desole, M.S., O'Neill, R.D., Serra, P.A., 2013. Anal. Chem. 85, 10282–10288.
Roche, R., Salazar, P., Martín, M., Marcano, F., González-Mora, J.L., 2011. J. Neurosci. Methods 202, 192–198.
Routh, V.H., 2010. Sensors 10, 9002–9025.
Schulz, M.K., Wang, L.P., Tange, M., Bjerre, P., 2000. J. Neurosurg. 93 (5), 808–814.
Sokoloff, L., 1977. J. Neurochem. 29, 13–26.
Thévenot, D.R., Toth, K., Durst, R.A., Wilson, G.S., 1999. Pure Appl. Chem 71, 2333–2348.
Thorens, B., 2010. Diabetes Metab 36, S45–S49.
Tokumaru, O., Kuroki, C., Yoshimura, N., Sakamoto, T., Takei, H., Ogata, K., Kitano, T., Nisimaru, N., Yokoi, Y., 2009. Neurochem Res 34, 775–785.
Vaddiraju, S., Legassey, A., Wang, Y., Qiang, L., Burgess, D.J., Jain, F., Papadimitrakopoulos, F., 2011. J. Diabetes Sci. Technol. 5 (5), 1044–1051.
van de Beek, D., de Gans, J., Tunkel, A.R., Wijdicks, E.F.M., 2006. N. Engl. J. Med. 354, 44–53.

Vannucci, S.J., Maher, F., Simpson, I.A., 1997. Glia 21, 2–21.
Vannucci, S.J., Simpson, I.A., 2003. Developmental switch in brain nutrient transporter expression in the rat. Am. J. Physiol. – Endocrinol. Metab. 285, E1127–E1134.
Vasylieva, N., Barnych, B., Meiller, A., Maucler, C., Pollegioni, L., Lin, J.-S., Barbier, D., Marinesco, S., 2011. Biosens. Bioelectron. 26, 3993–4000.
Wagner, A.K., Fabio, A., Puccio, A.M., Hirschberg, R., Li, W., Zafonte, R.D., Marion, D. W., 2005. Crit. Care Med. 33, 407–413.
Wahono, N., Qin, S., Oomen, P., Cremers, T.I.F., de Vries, M.G., Westerink, B.H.C., 2012. Biosens. Bioelectron. 33, 260–266.
Wang, J., 1999. J. Pharmaceut. Biomed. Anal. 19, 47–53.
Watts, A.G., Donovan, C.M., 2010. Front. Neuroendocrinol. 31, 32–43.
Wilson, G.S., Gifford, R., 2005. Biosens. Bioelectron. 20, 2388–2403.
Wisniewski, N.A., Moussy, F., Reichert, W.M., 2000. Fresenius J. Anal. Chem. 366, 611–621.
Wisniewski, N.A., Reichert, W.M., 2000. Colloids Surf. B: Biointerfaces 18, 197–219.
Zhao, W., Xu, J.-J., Chen, H.-Y., 2006. Electroanalysis 18 (18), 1737–1748.